Spatio-Temporal analysis of PM$_{2.5}$ using MODIS, MISR and SeaWiFS imagery over Lahore division

By

SIDRA ASHRAF
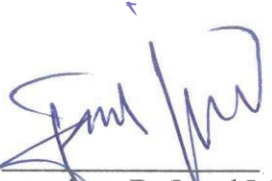
(2020-NUST-MS-GIS-329537)

A thesis submitted in partial fulfillment of the requirements for the degree of Master of Science in Remote Sensing and Geographical Information Systems

Institute of Geographical Information Systems School of Civil and Environmental Engineering National University of Sciences and Technology Islamabad, Pakistan

August-2024

THESIS ACCEPTANCE CERTIFICATE

Certified that final copy of MS/MPhil thesis written by **Sidra Ashraf (Registration No. MSRSGIS 00000329537), of Session 2020 (Institute of Geographical Information Systems)** has been vetted by undersigned, found complete in all respects as per NUST Statutes/Regulation, is free of plagiarism, errors, and mistakes and is accepted as partial fulfillment for award of MS/MPhil degree. It is further certified that necessary amendments as pointed out by GEC members of the scholar have also been incorporated in the said thesis.

Signature: _____

Name of Supervisor: Dr Javed Iqbal

Date: 26.1.24

Dr. Javed Iqbal
Professor & HOD IGIS. SCEE (NUST)
H-12, Islamabad

Signature (HOD): _____

Date: 26-1-24

Dr. Javed Iqbal
Professor & HOD IGIS. SCEE (NUST)
H-12, Islamabad

Signature (Principal & Dean SCEE): _____

Date: 12 FEB 2024

PROF DR MUHAMMAD IRFAN
Principal & Dean
SCEE, NUST

Academic Thesis: Declaration of Authorship

I, **<u>Sidra Ashraf,</u>** declare that this thesis and the work presented in it are my own and have been generated by me as the result of my original research.

"Spatio-temporal analysis of PM$_{2.5}$ using MODIS, MISR and SeaWiFS imagery over Lahore division".

I confirm that:

1.   This work was done wholly by me in candidature for an M.S. research degree at the National University of Sciences and Technology, Islamabad.

2.   Wherever I have consulted the published work of others, it has been attributed.

3.   Wherever I have quoted from the work of others, the source has been always cited.

4.   I have acknowledged all main sources of help.

5.   Where the work of the thesis is based on work done by myself jointly with others, I have made clear exactly what was done by others and what I have contributed myself.

6.   None of this work has been published before submission. This work is not plagiarized under the H.E.C. plagiarism policy.

Signed: ……………………………

Date: ………………………………

ACKNOWLEDGMENTS

TABLE OF CONTENTS

LIST OF FIGURES

LIST OF TABLES

LIST OF EQUATIONS

LIST OF ABBREVIATIONS

PM = Particulate matter

ECMWF = European center for medium range weather forecasts

MODIS = Moderate resolution imaging spectroradiometer

MISR = Multi imaging spectroradiometer

Sea Wifs = Sea-viewing field-of-view sensor

AOD = Aerosol optical depth

AERONET = Aerosol Robotic Network

SEDAC = Socioeconomic Data and application center

TOA = Top incident solar radiation

AQI = Air quality index

WHO = World health organization

ABSTRACT

Particulate matter ($PM_{2.5}$) is considered a major cause of mortality worldwide. In Pakistan, specifically in the industrial and capital city of Lahore, the air quality is so deteriorated that the provincial government closed schools and other institutions. A study was designed to (1) investigate the decadal trends of $PM_{2.5}$, urbanization, and (2) model metrological factors responsible for $PM_{2.5}$ over the Lahore division for the long period 1998-2019. The $PM_{2.5}$ temporal change was analyzed using the non-parametric Mann-Kendall trend test. Based on Mann Kendall test results Lahore division was divided into three regions: low, medium, and $PM_{2.5}$ polluted sites to know urbanization change through non raster Mann Kendall test. The impact of metrological factors was analyzed by multiple linear regression. The results highlighted that all the cities except Nankana sahib experienced a significant ($p \leq 0.05$) increase in this period, with highest values of 113 μgm^{-3} and lowest values of 49 μgm^{-3}. The air quality of the Lahore division was worse in Lahore, Okara and some parts of Sheikhupura and Kasur, showing the highest $PM_{2.5}$ concentrations of 113 μgm^{-3}. Urbanization in low $PM_{2.5}$ polluted site showed no significant ($p \geq 0.05$) trend with Z=-1.04, tau=0.33, P=0.29, sens slope=809 moderate $PM_{2.5}$ polluted site showed increasing trend with Z=2.08, tau=1, P=0.03, sens slope=1506 while high $PM_{2.5}$ polluted site showed increasing trend with Z=2.5, tau=3, P=0.01, sens slope=3236 respectively. The correlation coefficients of $PM_{2.5}$ concentration with temperature, wind speed, and precipitation are -0.53, -0.41 and -0.65, respectively, showing strong negative correlations. The correlation coefficients of $PM_{2.5}$ concentration with relative humidity and pressure was 0.69, showing positive correlation and 0.28, respectively. Multiple linear regression showed that metrological factors have 82% tendency to alter the concentrations of $PM_{2.5}$.

INTRODUCTION

1.1 Background Information

In the last few decades, one of the greatest social and ecological issues concerning has been air quality degradation. Swiftly increasing urbanization, industrialization, burning of fossil fuels and changing metrological conditions control the concentrations of air pollutants in the atmosphere (Van et al., 2010). Among these pollutants $PM_{2.5}$, tiny airborne particles which has aerodynamic diameter less than 2.5um, is the most deleterious pollutant (Delfino et al., 2005) and has drawn research attention in recent years (Meng et al., 2016; Apte et al., 2015; Lelieveld et al., 2015; West et al., 2016). Research showed $PM_{2.5}$ particles interact with solar radiation as they absorb and scatter. When absorption occurs the atmosphere gets warm, while it has a cooling effect when it causes high albedo. $PM_{2.5}$ is acknowledged to have adverse effects on public health and global climate (Brauer et al., 2016). $PM_{2.5}$ affects air quality and as a result, causes health issues and reduces visibility (Deng et al., 2012; Wang et al., 2015; Cheng et al., 2015; Yu et al., 2016 b).

It has been observed that $PM_{2.5}$ is the main precursor of smog and haze (Wang et al., 2016b). The prevalence of smog has been well- documented in numerous prominent cities worldwide, including Beijing, Delhi, Lahore, Mexico City, Los Angeles, and Tehran (Chen et al., 2013; Mohammadi et al., 2012; Shabbir et al., 2019). It is said that Lahore and Delhi are divided by borders but united in smog. Depending on the emission sources, chemistry of the atmosphere, and meteorological events, it's physical size distribution and chemical composition change over time and space (Seinfeld and Pandis, 2016).

1.2 Sources of Particulate Matter (PM$_{2.5}$)

Inorganic ions, carbonaceous molecules (black and organic carbon, including secondary organic aerosol), and mineral dust comprise the vast majority of PM$_{2.5}$ mass. The sources of emissions encompass various factors, including direct emissions such as forest fires and agricultural waste burning (Yokelson et al., 2009; Johnston et al., 2012) windblown mineral dust originating from arid regions (Reid et al., 2003), and inefficient fuel combustion (Bond et al., 2007). Additionally, secondary emissions arise from atmospheric chemical interactions involving primary gas-phase pollutant precursors. The precursors are released through a variety of processes, including both combustion and no combustion activities. Since air parcels are the primary carriers of air pollutants, it is assumed that all the stubble fires and crop residue burning in Delhi are to blame for the air pollution problems in the Lahore division. These activities encompass domestic energy consumption, the operation of cars on and off the road, energy production, solvents, industrial operations, and agricultural fertilizers. The chemical synthesis of PM$_{2.5}$ mass in the atmosphere exhibits a highly non-linear behavior once it is discharged (Womack et al., 2019; Lu et al., 2019). Various factors, including local environmental conditions, dominant sources, and the number of emissions from these sources influence the overall mass and chemical composition of PM$_{2.5}$. This complexity arises from the multitude of sources and the intricate chemistry involved in the creation of PM$_{2.5}$. Furthermore, since political boundaries do not constrain air pollution and atmospheric chemistry do not constrain air pollution (Liang et al., 2017; Zhang et al., 2018; Meng et al., 2019), it is necessary to consider the transboundary impacts when implementing measures to mitigate these issues. This requires a comprehensive understanding of the contributions of PM$_{2.5}$ sources and the associated disease burden at various scales, ranging from sub-national to global levels. The Lahore division had numerous instances of smog and haze, which demonstrated the highly unhealthy air quality. So, research aims to identify the spatiotemporal trend and to evaluate the

effect of metrological factors (wind, temperature, relative humidity, pressure, precipitation) on PM$_{2.5}$ concentrations.

1.3 Factors affecting on particulate matter (PM$_{2.5}$)

Identifying the key determinants of PM$_{2.5}$ is of utmost importance in the field of PM$_{2.5}$ pollution study. Various elements, encompassing emissions, climatic conditions, and geographical location influence the concentrations of PM2.5. Meteorological conditions exhibit a strong correlation with the dispersion, buildup, and transmission of PM$_{2.5}$ particles (He et al., 2017; Hu et al., 2021). Extreme polluting events over urban areas are not due to unexpected rise of discharge of pollutants but because of favorable meteorological conditions (Ziomass et al.1995). Contribution to the transport, accumulation and distribution of air pollutants are analyzed in the form of meteorological circulations and meteorological factors also represent the weather conditions, such as wind speed, surface temperature and humidity (relative and absolute) precipitation (Cheng et al., 2007; Ding et al., 2009). High intensity of pollution incidents over Hong Kong were studied through examining the influence of relative humidity, temperature, intensity of solar radiation, wind direction and speed (Tenner and Law 2002). Meteorological factors directly or indirectly affect PM$_{2.5}$ concentrations (Chen et al., 2020). Pakistan has a large geographical area and diverse climates, hence PM$_{2.5}$ pollution varies by region. Thus, PM$_{2.5}$ and meteorological elements must be studied in each region. Therefore, the Lahore division's various climates contribute to frequent haze vents. This research aims to assess the impact of metrological variables on PM$_{2.5}$ in the Lahore administrative region. The factors are defined as follows:

1.3.1 Metrological factors.

Pressure is described, the force that a unit of area experiences due to the weight of air molecules in the Earth's atmosphere is referred to as air pressure. Usually, it is expressed in terms of

millimeters of mercury (mmHg), pascals (Pa), or atmospheres (atm). At sea level, the typical atmospheric pressure is roughly 101.3 kilopascals (kPa), or 1 atmosphere.

Wind speed is generally calculated using U and V wind components. U component of wind shows the part of the wind that flows eastward. It's how fast air is moving horizontally toward the east. A negative sign represents the air going toward the west. V component of wind shows the part of the wind that blows northward. Air moving toward the north is moving at this speed. A negative sign represents the air going toward the south.

Atmospheric temperature. The unit is Kelvin. Kelvin temperature is converted to °C by subtracting 273.15. This parameter is observed at many atmospheric levels.

Precipitation in question refers to the cumulative precipitation that is deposited on the Earth's surface. This precipitation is produced by the cloud scheme inside the ECMWF Integrated Forecasting System (IFS). The cloud scheme is a represents of the processes involved in the development and dissipation of clouds and the occurrence of significant precipitation on a broad scale. Variations influence these processes in atmospheric properties, including pressure, temperature, and moisture. The cloud scheme predicts these variations at geographic scales equal to or greater than the size of a grid box. The convection method implemented in the IFS can generate precipitation through convective processes occurring at smaller geographical scales than the grid box. The metric is aggregated within a specific temporal interval, contingent upon the retrieved data. In the reanalysis process, the accumulation period refers to the duration of one hour that concludes at the specified validity date and time. The parameter is measured in meters of water equivalent, representing depth.

Top atmospheric radiation refers to the solar radiation received from the Sun, also known as shortwave radiation, at the uppermost layer of the Earth's atmosphere. The term "horizontal plane"

refs to a flat surface that is parallel to the ground. In the context of radiation, the phrase "amount of radiation passing through a horizontal plane" pertains to measuring the quantity of radiation that traverses this specific plane. The metric is aggregated within a specific temporal interval, contingent upon the retrieved data. In reanalysis process, the accumulation period refers to the duration of one hour, specifically terminating at the validity date and time.

Surface solar downward radiation measures the shortwave solar energy that reaches a horizontal plane on Earth. This metric includes direct and diffuse sun radiation. Shortwave solar radiation is partly reflected to space by clouds and aerosols and partly absorbed. The rest is Earth-surface event. This parameter is approximately the model equivalent of what a surface pyranometer would measure. When comparing model parameters with observations, remember that observations are typically limited to a location in space and time rather than averages over a model grid box. Data extracted determines this parameter's accumulation period. The accumulation duration for reanalysis is over 1 hour terminating at the validity date and time. Ensemble members, mean, and spread accumulate over the 3 hours ending at the validity date and time. Joules per square meter

Relative Humidity is the water vapor pressure as a percentage of the air saturation point. Saturation over water is computed at temperatures above 0°C (273.15 K). Calculated for saturation on ice below -23°C. This characteristic is produced by quadratic interpolation between ice and water values between -23°C and 0°C.

LITERATURE REVIEW

The emerging ability of satellite remote sensing data provides an unprecedented opportunity to develop the understanding and linkage of aerosol air quality and climate change (Zhang and Reid, 2010; Yoon et al., 2012; Luo et al., 2014; He et al., 2016). Mapping aerosol distribution using satellite remote sensing is an efficient way to understand the aerosols' worldwide spatial and temporal character. Using data from polar orbiting satellites like Advanced Very High-Resolution Radiometer (AVHRR), Moderate Resolution Imaging Spectroradiometer (MODIS), Multi-angle Imaging

Spectroradiometer (MISR), and Sea-viewing Wide Field-of-view Sensor (SeaWiFS), (Kaufman et al., 1997; Remer et al., 2005; Mischenko and Geogdzhayev, 2007; Kahn et al., 2005, 2010, Jackson et al., 2013) several algorithms have been developed to retrieve aerosol optical depth (AOD). Aerosol Optical Depth (AOD) is a quantitative estimate of the amount of aerosol present in the atmosphere, and it can be used as a proxy for surface Particulate Matter $PM_{2.5}$ (particles smaller than 2.5 μm median diameter) Different satellite sensors provide different AOD values because of different sensor characteristics and retrieval algorithms.

Badarinath et al. (2009b, 2009c) investigated the long-range transport of biomass burning aerosol, generated from area 1600 km far from its research site at Hyderabad (India) using satellite and ground based remote sensing data. A statistically important positive trend of AOD found with seasonal adaptability using data of Aerosol Radiative Forcing over India (ARFINET) (Babu et al., 2013)

6

Ahmad et al. (2023) did a research investigation pertaining to the persistence of PM $_{2.5}$. The researchers collected samples of PM $_{2.5}$ at urban locations in Lahore during both the winter and summer seasons of 2019. The average concentration of $PM_{2.5}$ throughout winter and summer seasons in Lahore exceeds the national environmental quality standards (NEQS) of Pakistan and the World Health Organization (WHO) by factors of

15 and 4.6, respectively. The primary constituents of PM2.5 were carbonaceous species. During both winter and summer seasons, strong correlation was seen between metallic and carbonaceous species and the creation of OH radicals. This correlation indicates that the emissions from vehicles, coal burning, and industrial activities had a significant role in the generation of OH radicals.

In their work, Zhang et al. (2020) investigated the dynamics of PM2.5 in 33 megacities using long-term remotely sensed measurements. The researchers also analyzed the study region in relation to population density. Areas with higher population density had elevated levels of $PM_{2.5}$ concentrations. Furthermore, megacities in these areas displayed higher $PM_{2.5}$ than those in moderately and sparsely populated regions. The regions with the highest levels of pollution are China, India, and South Asia, whereas Europe and Japan are among the least polluted regions. It is worth noting that none of the 33 megacities currently meet the World Health Organization's $PM_{2.5}$ attainment class, which sets a limit of less than 10 $\mu g/m^3$. Conversely, 9 megacities fall into the $PM_{2.5}$ nonattainment class, exceeding the 35 $\mu g/m^3$threshold. This observation suggests that the high population density in these areas is a significantly contributes to air pollution.

The utilization of Geographic Information Systems (GIS) has facilitated the process of determining the Mann-Kendall trend for $PM_{2.5}$. Additionally, mapping methodologies

have been employed to discern the geographical areas characterized by air quality deemed exceptionally detrimental to human health. This methodology allows for the assessment of the impact of meteorological variables on the levels of $PM_{2.5}$. The utilization of interpolation techniques facilitates the determination of wind direction, hence aiding in the identifying of the transboundary dispersion patterns of pollutants.

The mortality rate associated with $PM_{2.5}$ exposures had a significant increase from 82,300 in 1990 to 135,100 in 2015, encompassing all age groups and genders (Mukhtar, 2018). Smog and haze incidents occurred frequently in the Lahore division, demonstrating the dismal air quality. $PM_{2.5}$ haze are tiny particles that can enter the bloodstream leading to cardiovascular and respiratory diseases and other health issues (Penner et al., 2004; Li et al., 2007; Tollefson, 2010; Kaufman et al., 2002). According to estimates from the World Health Organization (WHO), in 2000, urban areas worldwide lost 6.4 million healthy years of life and 800,000 lives due to exposure to ambient $PM_{2.5}$ (Cohen et al., 2004). The NASA team found that $PM_{2.5}$ exposure caused 2.89 million premature deaths in 2019— 1.19 million from heart disease, 1.01 million from stroke, 287,000 from COPD, 230,000 from lower respiratory infection, and 166,000 from lung cancer. They estimated that 43% of those deaths happened in China and 23% in India, two of the world's most populous and polluted nations. Pakistan, Bangladesh, and Nigeria also had high $PM_{2.5}$ exposure and many premature deaths, although none of these nations accounted for more than 3% of $PM_{2.5}$-related mortality.

MATERIALS AND METHODS

3.1 Study Area

3.1.1 Geography and Landscape

The study primarily focuses on the Lahore Division, is an administrative division within the Punjab Province of Pakistan. The region has five districts: Kasur, Lahore, Nankana Sahib, and Sheikhupura. The cumulative land area of the division amounts to 11,727 square kilometres and geographically situated within the coordinates of 31°15′—31°45′ N and 74°01′—74°39′ E. Lahore is bordered to the north and west by the Sheikhupura District, to the east by Wagah, and to the south by Kasur District shown in figure 2.1. The population density is 1,700 individuals per square kilometers.

3.1.2 Climatic Variations

Division has a tropical semi-arid climate, which is marked by humid and lengthy summers that are unusually hot average temperatures during this period can range from 30°C to 40°C (86°F to 104°F) or even higher. The winters in this region are dry and mild with average temperature ranging from 5°C to 15°C (41°F to 59°F). Fog can be a common occurrence during the winter months, leading to reduced visibility and disruption of transportation. The area experiences monsoon rains as well as dust storms. Climate variations can be influenced by larger-scale climatic phenomena, such as El Niño and La Niña, in addition to long-term trends in climate change. Moreover, the process of urbanization and changes in land use within the Lahore Division might exert an impact on its microclimate.
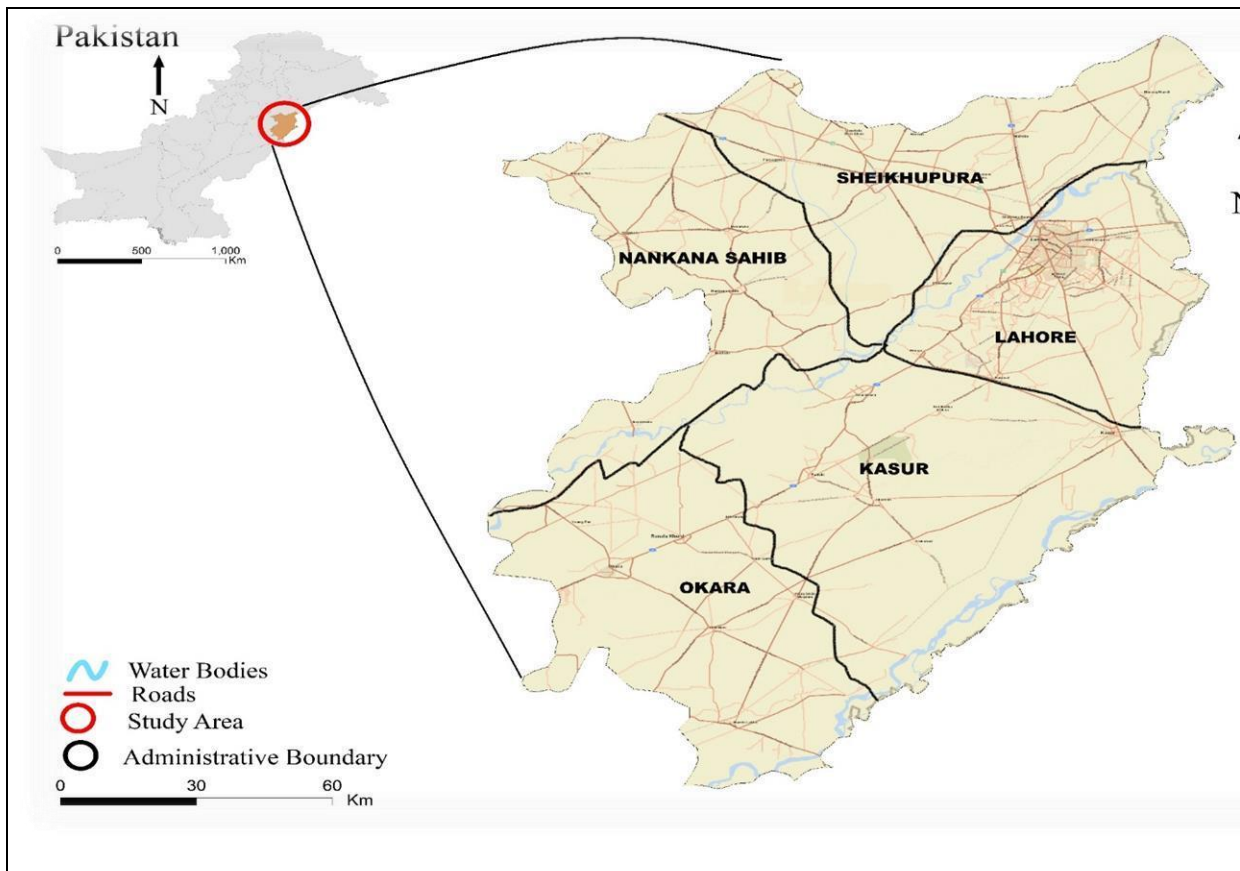
Figure 3.1. The study area consists of five cities Sheikhupura, Lahore, Kasur, Okara and Nankanasahib from Lahore division.

3.2　Dataset

For this study three remote sensing data sets were used, as shown in table 2.1. The main data set was annual grids of $PM_{2.5}$ from MODIS, MISR and SeaWiFS Aerosol Optical Depth (AOD) consisting of annual concentrations (micrograms per cubic meter) of all composition ground-level fine particulate matter ($PM_{2.5}$). This data set combines AOD retrievals from NASA MODerate resolution Imaging Spectroradiometer Collection 6.1 (MODIS C6.1), Multi-angle Imaging Spectroradiometer Version 23 (MISRv23), MODIS Multi-Angle implementation of Atmospheric Correction Collection 6 (MAIAC C6), and SeaWiFS Deep Blue Version 4. By utilizing the GEOS-Chem chemical transport model, we can connect this total column measure of aerosol to the concentration of $PM_{2.5}$ close to the Earth's surface. Geographically Weighted Regression (GWR) predicts and adjusts for residual $PM_{2.5}$ bias per grid cell in satellite-derived results using global ground-based WHO observations. Estimates are mostly for large-scale investigations. Providing gridded data sets with a resolution of 0.01 degrees enables users to aggregate data in a way that best suits their specific purposes. This data is derived from SOCIOECONOMIC DATA AND APPLICATIONS CENTER(SEDAC) from 1998 to 2019.

Metrological data obtained from ERA 5 for the year ranging from 1998 to 2019 is shown in table 2.2. Gridded monthly reanalysis data of single level at 0.25 degrees was used. land sat imageries for Land Use Land Classification was obtained from Google earth engine after 10 years of interval. For the year 1998 and 2008 land sat 5 imageries with resolution of 30km was used. For the year of 2019 land sat 8 imagery was used.

11

The spatio-temporal distribution of aerosols' abundance, chemical, physical, and optical properties is challenging for their characterization and is a limitation while acquiring data through direct observation (Liu et al., 2016). To resolve this issue, ground-based networks for aerosol measurement have been established around the globe for procuring constant datasets related to aerosol parameters over land and ocean like the Aerosol Robotic Network (AERONET) (Holben et al., 1998). NASA established AERONET but that required large amount of manpower and proper maintenance, which can ultimately result in limitation in building a valuable database (Kang et al., 2016). AERONET version 3 of level 2 at 500nm height for the period from 2007 to 2019 was used to validate Raster AOD.

The study aims to find spatio temporal changes of $PM_{2.5}$ from the year 1998 to 2019 using Mann Kendall test and to determine the significant sources of this pollutant in the division of Lahore where smog has been declared as a fifth season. furthermore, effects of metrological factors on the levels of $PM_{2.5}$. Results of trend will enable us to identify the cities with extremely poor air quality.

3.3 Methods

After transformation to same spatial and temporal resolution, comparative assessment was carried out with all data sets. $PM_{2.5}$ annual grids were preprocessed (cloud removal, dust clipping, etc.), and AERONET data was converted to yearly sets. After that, raster AOD and ground AOD were revalidated (while the grids have already been validated by WHO), as shown in figure2.2. Validated annual $PM_{2.5}$ trends were analyzed. Mann Kendall (Mann, 1945; Kendall, 1975) trend test was used over all validated grids to determine any statistically significant change with time.

Table 3.1 Dataset used in the study along with their specifications.

DATA	TIMEPERIOD	SOURCE	RESOLUTION
AERONET	2007-2019	https://aeronet.gsfc.nasa.gov/ (Aerosol Robotic network)	-
Annual product of $PM_{2.5}$	1998-2019	Socioeconomic Data and Applications Center(sedac)	0.01
Landsat	1998-2019(after 10 year)	Earth data	30 m
Metrological factors	1998-2019	ERA-5	0.25 degrees

Table 3.2. Descriptions of meteorological factors used in this study acquired with a spatial resolution of 0.125o at noon (1200 hrs).

Metrological factors	Unit	Description
Relative humidity	%	Relatively humidity at 1000 hPa pressure level
Pressure	Pa	Pressure is described, the force that a unit of area experiences due to the weight of air molecules.
U wind speed	m/s	Horizontal air moving speed at 100 meters towards the east.
V wind speed	m/s	Horizontal air moving speed at 100 meters towards the north.
Temperature	K	Temperature in the atmosphere.
Precipitation	$kg\ m^{-2}\ s^{-1}$	cumulative precipitation that is deposited on the Earth's surface.
Surface solar downward radiation	Jm^{-2}	measures the shortwave solar energy that reaches a horizontal plane on Earth.
TOA incident solar radiation	Jm^{-2}	solar radiation received from the Sun at the uppermost layer of the Earth's atmosphere.

Mann-Kendall trend test is a non-parametric test and had been used in trends for time series of

hydro climatological (e.g., Partal and Kahya, 2006; Jiang et al., 2007; Tabari and Hosseinzadeh

Talaee, 2011; Reiter et al., 2012; Wang et al., 2012). Non-parametric methods are better as

compared to parametric trend determination method because they are less sensitive to outliers

Wang, (2006). Man, Kendall trend test is a rank-based method that assesses the null hypothesis

of time series datasets by categorizing it to randomness or no trend. Hrisch., et al., (1981) and

Khattak., et al. (2011) explained the Mann-Kendall process as follows:

$S = \sum_{k-1}^{n} {}^{1} \sum_{j=k+1}^{n} \text{sgn} (xj - xk)$ .... Eq 1

$i \quad if (xj - xk) > 0$
$\text{sgn} (xj - xk) [0 \quad if (xj - xk) = 0] -1 \quad if (xj$
$- xk) < 0$

In equations (1) n represents the time series length, xj and xk are the sequential data and S is testing

statistics. An upward trend is identified by the positive value of S and a downward trend by the negative

value of S. For long time series (n >10), S statistic tends to normality along with expectation (E) and variance

(Var). These can be represented in exponential form as:

$E(S) = 0$ .... Eq. 3

$\text{Var(S)} = \frac{1}{18} [n(n - 1) (2n + 5 - \sum_{p-1}^{q} tp (tp - 1)(2tp + 5))]$ .... Eq. 4

In the above equation tp is the number of observations in the pth tied group and qth is the number of tied

groups in the time series. The standardized test statistic (ZMK) can be calculated as follows:
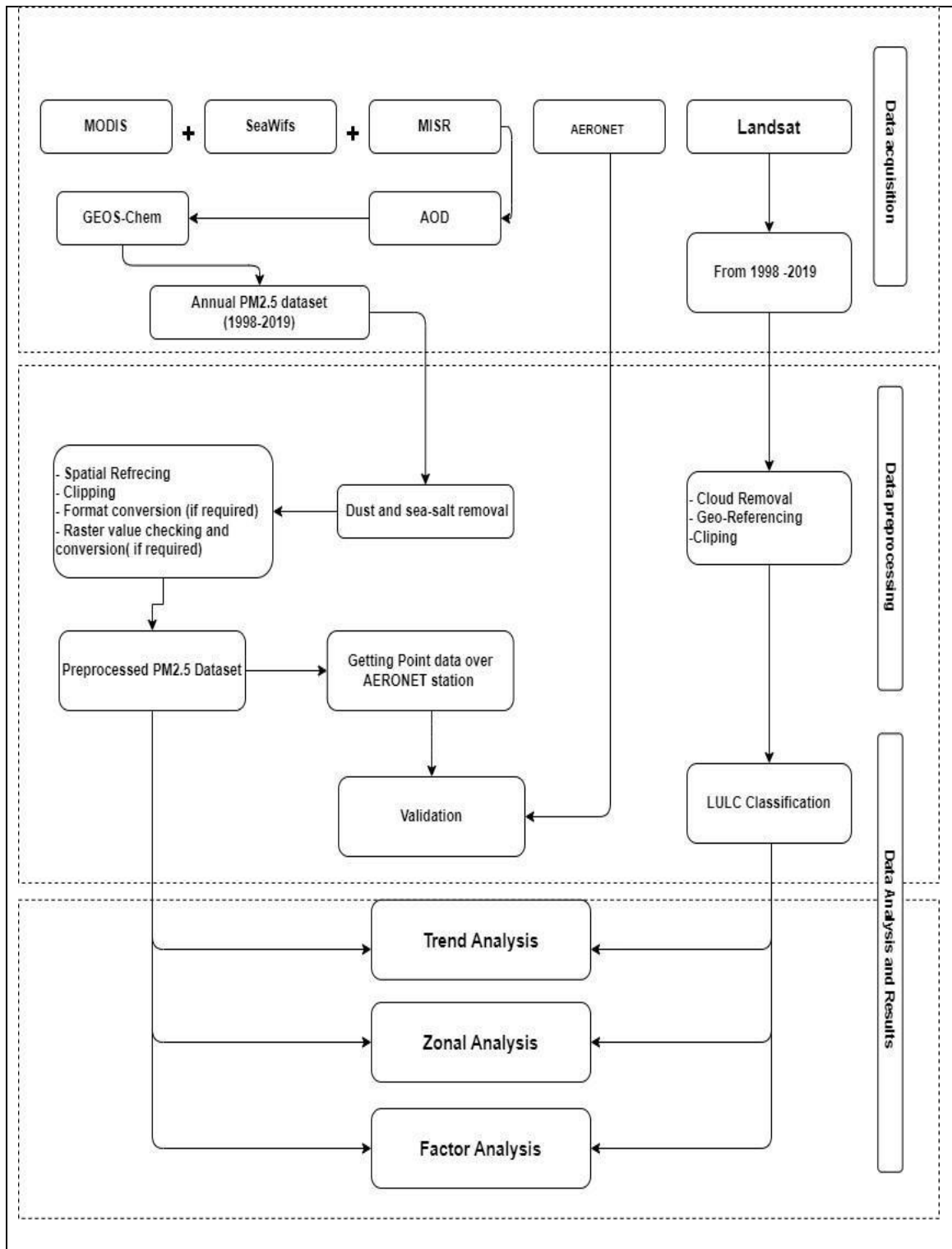
Figure 3.2 Methodological Framework showing data acquisition, data preprocessing and data analysis and results.

$$Z_{MK} = \begin{cases} \dfrac{S-1}{\sqrt{Var(S)}} & if\ S > 0 \\ \dfrac{S+1}{\sqrt{Var(S)}} & if\ S < 0 \\ 0 & if\ S = 0 \end{cases} \quad\text{... Eq.5}$$

The standardized test statistic (ZMK) for Mann-Kendall follows a standard normal distribution. The ZMK is related to a probability-value (p-value = observed significance level) of a trend calculating the evidence against the null hypothesis. The strength of trend against the null hypothesis will be greater when p-value is smaller. A two-tailed standardized table can be used to obtain the corresponding p-value (Nasri and Modarres, 2009). In this study, Mann Kendall trend test was applied to entire datasets.

From 1998 to 2019, land use land classification was conducted using Landsat imagery acquired after a 10-year gap (i.e., 1998,2008,2019). LU/LC was performed on Google Earth Engine.In remote sensing Normalized difference indices are utilized to analyze and classify surface cover types. The premise of the Normalized Difference Built-up Index (NDBI), which was proposed by Zha in 2003, is a method used to extract urban surfaces. It is defined as...

$$NDBI = \frac{Band5-Band4}{Band5+Band4} \quad\text{-------------------------------Eq.6}$$

Urbanization class was extracted, and non-raster Mann Kendal trend test was applied to know how this class is playing role in changing $PM_{2.5}$ trends. The Lahore district is characterized by widespread industrialization. $PM_{2.5}$ pollution originates from a wide variety of industries, including steel, rubber, coal power stations, brick kilns, and building sites (Ahmad et al., 2020).

These industries were digitized using QGIS interface.
The presence of a heavy $PM_{2.5}$ pollution burden in the air is thought to be the primary catalyst for smog formation, and studies show that smog is more common in the winter (shah et al.,2019).

Metrological factors which include pressure, windspeed, temperature, precipitation, top surface atmospheric radiations, surface solar downward radiations, and relative humidity were obtained from ERA 5 it is reanalysis of monthly data which was aggregated to yearly data using mean of four winter months (October, November, December, January) which showed higher levels of $PM_{2.5}$ burden in air.

Because two raster data sets must have the same projection and resolution, preprocessing steps were taken to bring metrological data sets such as pressure, windspeed, temperature, precipitation, top surface atmospheric radiations, surface solar downward radiations, and relative humidity raster up to the same resolution (0.01) and number of cells (15214) as of $PM_{2.5}$ grids. After ensuring consistency between the $PM_{2.5}$ grids and the raster of metrological variables, we used the same projection (GCS_WGS_1984) and resolution (0.01). A correlation between all such factors was found to determine which meteorological component is most strongly connected with $PM_{2.5}$. Multiple linear regression was used to evaluate the relationships between the various variables and $PM_{2.5}$ concentration levels. MLR was conducted for 1998, 2008, 2019 and mean of all years between 1998-2019.

Wind direction plays a pivotal role in the transmission of $PM_{2.5}$ pollution. The U and V component of wind was obtained from ERA 5 for the year 1998, 2008, 2019. Only 4 winter months mean was considered October, November, December, and January. Literature showed that these months have higher levels of $PM_{2.5}$ pollution than summer months. Wind direction was estimated using GRASS AND QGIS software.

RESULTS AND DISCUSSIONS

This section deals with the results which are achieved from working methodology used to know significant sources of $PM_{2.5}$ and the effect of metrological factors on the concentrations of $PM_{2.5}$ once entered in the atmosphere.

4.1 Validation of raster data with ground data.

A correlation matrix was formulated considering the number of observations at 0.05 probability shown in Table 4.1. The value of ground observed AOD at 480 nm with raster AOD was 0.561 which was highly significant according to the Pearson coefficient table. Meanwhile, ground observed AOD at 500nm with raster AOD was 0.368 which was non-significant.

4.2 Trend analysis of PM $_{2.5}$

Mann Kendall trend analysis was done over the yearly aggregated data set through R language. Probability and trend surface was generated, as shown in Figure 4.1 (b). The Mann Kendall test tells whether the trend is increasing or decreasing with time and the probability value tells whether trend is increasing significantly or non-significantly shown in Figure 4.1 (a).

If the value is less than 0.05, it means change is significant. Most parts of the Lahore, Sheikhupura, Okara and Kasur have shown a significantly increased trend with 113 ug/m^3 values and Major part of Nankana Sahib have shown a significant decreased pattern of $PM_{2.5}$ with 49 ug/m^3 and minor part is showing a non-significant decreased pattern.

Table 4.1. Shows correlation matrix between raster and ground AOD.

Data Type	AOD_480nm	RASTER_AOD	AOD_500nm
AOD_480nm	1		
RASTER_AOD	0.561 *	1	
AOD_500nm	0.848*	0.368 ns	1

N= 13 year; p =<0.05; *= significant at 0.05; ns= non- significant

4.3 Land use land classification to extract Urbanization.

Basic purpose for LU/LC was to extract urbanization class which is believed to be a contributing factor for $PM_{2.5}$.LU/LC was done for the years 1998(a),2008(b) and 2019(c) as shown in Figure-4.2. The kappa coefficients were 94%,93% and 96% simultaneously. Urbanization class was extracted from the LU/LC for the years 1998(a), 2008(b) and 2019(c) as shown in Figure 4.3. The study area was divided into three regions according to $PM_{2.5}$ trend and keeping in mind the Punjab air quality standards low, medium, and high polluted $PM_{2.5}$ sites respectively shown in Figure 4.8.

Non raster Mann Kendall and Sens slope test was applied. The Mann Kendall test tells whether the increase is positive or negative, and Sens slope tells the magnitude with which change is occurring. Results showed that urbanization has gradually increased from the years 1998 to 2008 and 2019. It was noted from the probability value that Low polluted $PM_{2.5}$ has shown no significant trend for urbanization (z= -1.044, tau=0.33, p=0.29) whereas Sens slop value tells us the change in urbanization was about 809. Probability value for medium (z= 2.088, tau=1, p=0.03)

and high polluted $PM_{2.5}$(z=2.556, tau=3, p=0.015) has shown a significant increasing trend with Sens slope of 1506 and 3236 respectively shown in table. Results showed areas with high urban sprawl in Lahore and Okara have high $PM_{2.5}$ pollution. So, urbanization could be one of the main contributors to $PM_{2.5}$ pollution in the atmosphere.

4.4 Industrialization

The spatial locations of different industries and brick kilns are shown in Figure 4.4. Most of these industrial units are located within 20km distance of residential areas. Many industries are registered within Lahore division and produce different emissions that degrade air quality. An inventory of different categories of Industries in Lahore division and their emissions is given in Table 2. 2. These emissions have been determined using the European Environmental Agency (EEA) emission inventory guidebook 2019. It was noted from the table that plastic, paper manufacturing, power plants, steel, wood, leather construction, ceramics, textile, rice industries are the main contributors for $PM_{2.5}$ pollution. Mainly these industries are in Sheikhupura, Lahore and Okara. A significant trend for $PM_{2.5}$ is observed in these cities, so industries are one of the contributing sources for $PM_{2.5}$ in the atmosphere. Increased urbanization leads to industrialization, producing many air pollutants, but our main concern is with $PM_{2.5.}$

4.5 Correlation analysis of metrological factors

As it is already mentioned in methods using GRASS GIS 7.0.3 version multi-variate correlation was estimated for raster's with the help of library r.covar . To better understand correlation between $PM_{2.5}$ and metrological factors, the correlation coefficients of $PM_{2.5}$ and each metrological factor were calculated between the 1998 to 2019 years. As shown in Table 4.3, $PM_{2.5}$ concentrations positively correlate with pressure and relative humidity and negative correlation with temperature, precipitation, wind speed. The correlation coefficients of $PM_{2.5}$ concentration with temperature, relative humidity, and precipitation are -0.53, -0.69 and -0.65 respectively, showing strong negative correlations. The correlation coefficients of PM2.5 concentration with wind speed and pressure are

-0.41 and 0.28 respectively. The correlation coefficients of $PM_{2.5}$ with surface downwelling radiations, top atmospheric solar radiations are 0.17 and 0.15 respectively, showing non-significant relationship. So, for further multiple linear regression wind speed, pressure, temperature, precipitation, and relative humidity was selected. Surface downwelling solar radiation and top atmospheric solar radiation showed no significant relation, so these both factors were excluded.
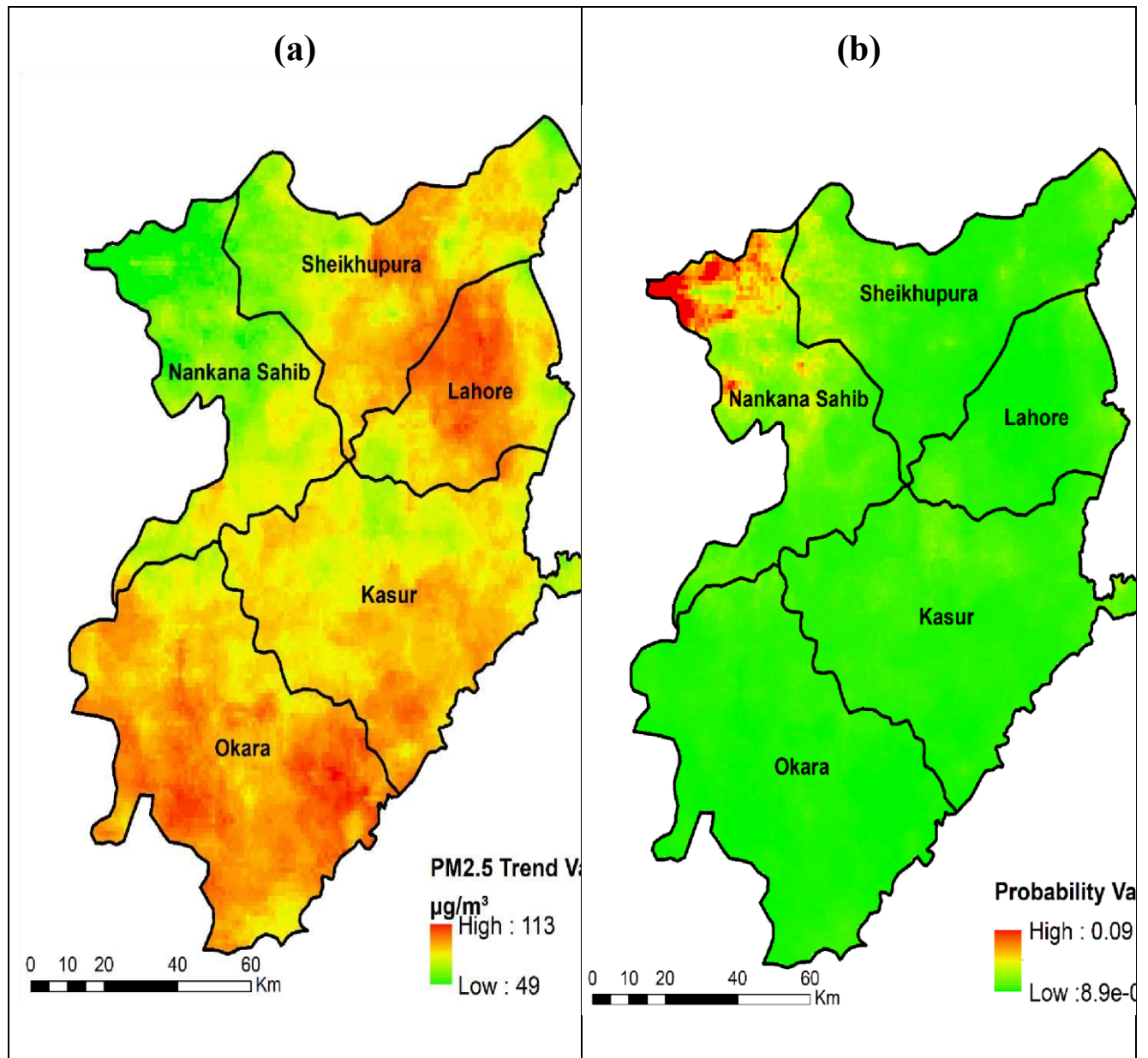
Figure 4.1. Displaying Mann Kendall trend for PM$_{2.5}$ and probability trend map (a) probability map(b).
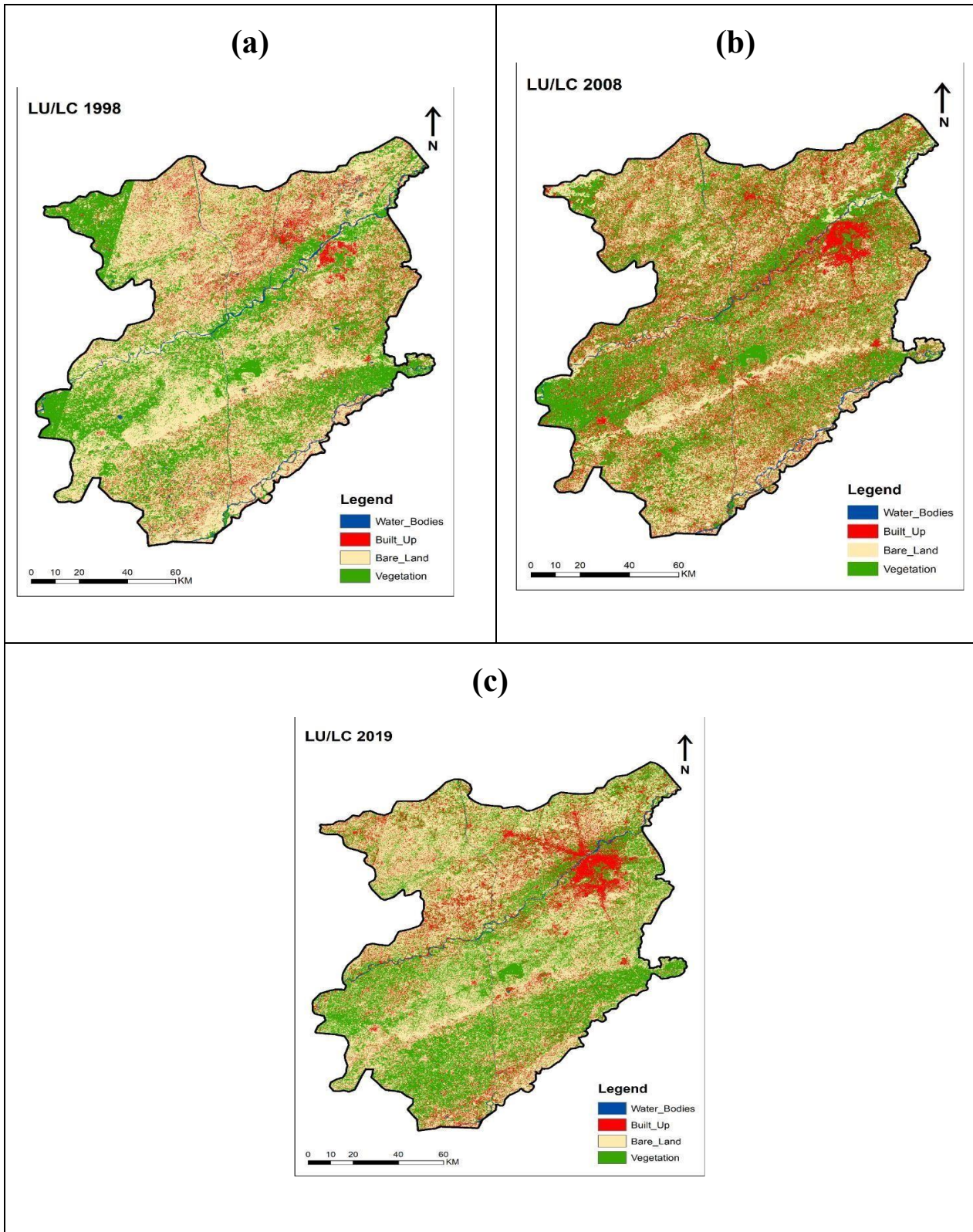
Figure 4.2. Presenting Land Use Land Cover for the year 1998 (a), 2008(b), 2019(c).
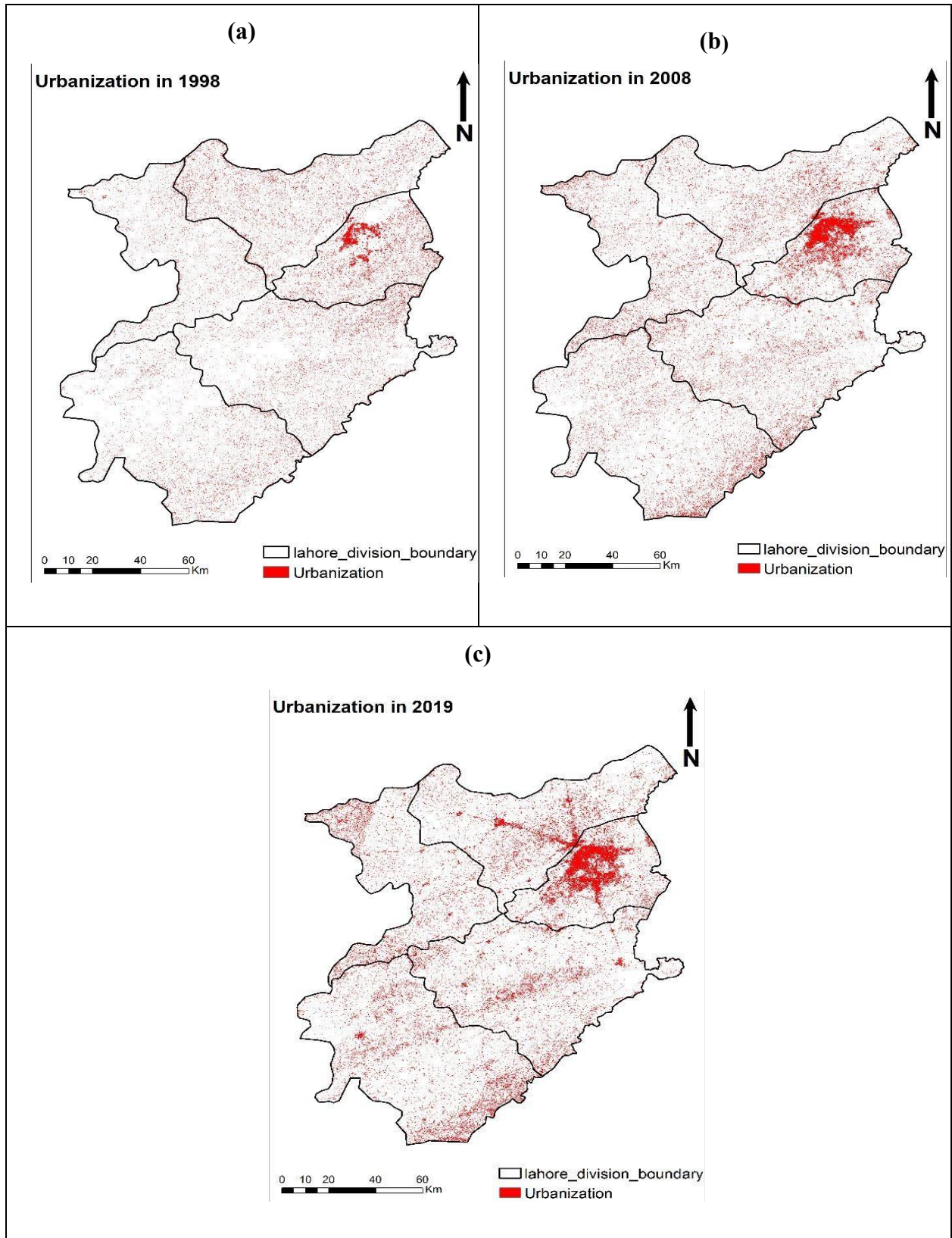
Figure 4.3. Showing extracted urbanization class for the year 1998(a), 2008(b), 2019(c).

Table 4.2. Showing results of non-parametric Mann Kendall trend test for urbanization in Lahore division.

Categories of site	Test Statistic (Z)	Kendall tau score	Probability value	Sens slope	Trend
Low PM2.5 polluted sites	-1.044	0.333	0.2962	809	No significant trend
Moderate PM2.5 polluted sites	2.088	1	0.0367	1506	increasing trend
Heavily PM2.5 polluted sites	2.556	3.00	0.015	3236	increasing trend
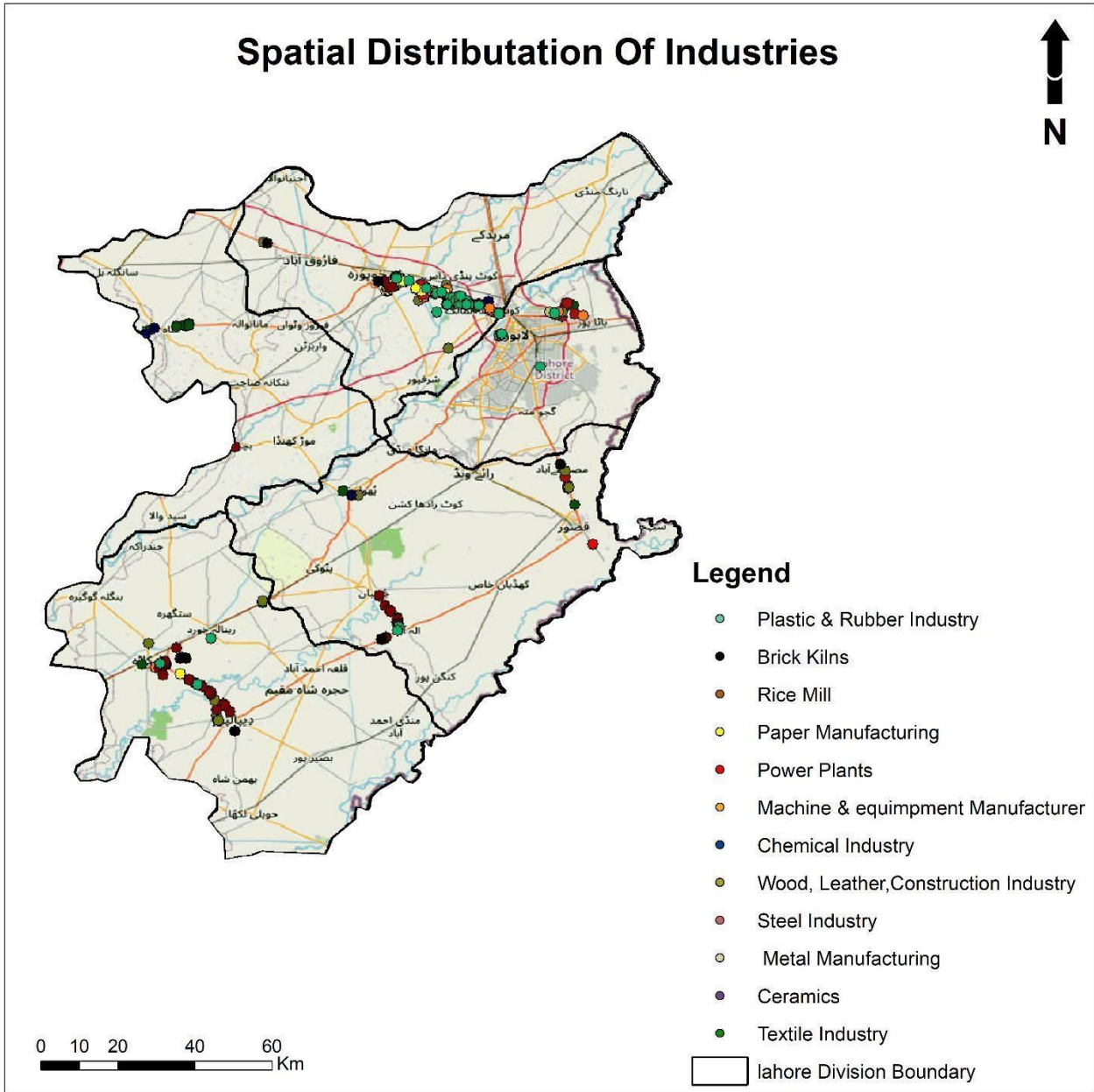
Figure 4.4 Presenting the industries in the Lahore division responsible for particulate matter PM$_{2.5}$ pollution.

4.6 Comparative assessment of multiple linear regression for monthly winter aggregated metrological factors.

r.multi regression_is designed for large datasets that cannot be processed in R. A p-value is therefore not provided, because even very small, meaningless effects will become significant with many cells.

Using r.multi regression extension in GRASS version 7.0.3 multiple linear regression was formulated for the years 1998,2008,2019 and overall from 1998 to 2019 . Results showed that for the year 1998 R square and adjusted R squared was 0.78, as shown in Table 4.3. which indicates that the model has 78% efficiency, and the factors have 85% effect on the concentrations of $PM_{2.5}$. Similarly, the year 2008 R squared and adjusted R squared was 0.80 shown in Table 4.4. which indicates that the model has 80% efficiency, and the concentrations of $PM_{2.5}$ in the atmosphere are affected 90% of these metrological factors. 2019-year results showed that R squared and adjusted R squared is 0.82 shown in Table 4.5 which means wind speed, pressure, precipitation, relative humidity, and temperature 82% explains the concentrations of $PM_{2.5}$ once entered in the atmosphere.

Overall multiple linear regression 1998 to 2019 results showed that R squared and adjusted R squared is 0.85 shown in Table 4.5, meaning 85 % metrological factors have tendency to affect the concentrations of $PM_{2.5}$. It was noted that overall model efficiency increased as the concentrations of $PM_{2.5}$ and other factors increased.

A residual and estimate map was generated by the software for every year. Residual tells us how far the results from the fitted line and estimate tells us how strongly dependent and independent factor is correlated. Estimate maps for 1998 have the highest value of 49ug/m^3 and lowest value

of 33.g ug/m^3.High values are shown in red color and low values in green. Values between high and low are shown in yellow color. Significant parts of Lahore and some parts of Sheikhupura, Okara falls under high value while most of the part of Sheikhupura, Okara and whole Nankana sahib falls in low value depicted by green color as shown in Figure 4.5 (a). It was observed mainly in lahore and some parts of Sheikhupura, Okara shows a strong relationship between PM$_{2.5}$ concentrations and metrological factors. The residual map shows high values shown with red color 5ug/m^3 and low values of -3.1 ug/m^3 shown with the green color in Figure 4.6(a). It is noted that major parts of Lahore, Sheikhupura, Kasur and Okara fall within the low range showing that results accurate and near to fitted line. Similarly, the year 2008 estimate map has a higher value of 63.5 and a low value of 44 ug/m3 shown in Figure 4.5 (b). Major part of Lahore and minor parts of Okara and Sheikhupura fall within high range while Nankana Sahib and major parts of Kasur, Sheikhupura and Okara fall within low range.

The residual map for 2008 showed higher values of 3.7 and lower values of -3.8 ug/m3. Major parts of Lahore, Sheikhupura and Kasur fall within lower values, showing that results are near to fitted line shown in Figure 4.6 (b).

The estimate map shown in Figure 4.5(c) for the year 2019 shows higher values of 60.2 ug/m3 and lower values of 40.3 ug/m3. Majorly Lahore, Kasur, and Okara falls with higher values depicted by red color which means PM$_{2.5}$ and metrological factors have strong relationship in these cities while Nankana sahib and Sheikhupura falls under low values showing weak relationship between dependent and independent factors. The residual map shown in Figure 4.6 (c) for the year 2019

shows higher values of 2.7 and lower values of -4.7 ug/m3. Most of the Lahore, Sheikhupura and Nankansahib fall within higher values means results are not accurate and away from fitted line. The estimate map shown in Figure 4.5 (d)from 1998 to 2019 shows higher values of 1304 ug/m^3 and lower values of 907.3 ug/m^3. The majority of Lahore half of the Okara and Kasur depicted by red color falls under high values. It shows that these cities have a higher relationship between PM2.5 and metrological factors. The residual map shown in Figure (d) from 1998 to 2019 shows higher values of 97.6 ug/m3 and low values of -67ug/m3 overall. It is noted that the majority of Lahore, Sheikhupura, Kasur and Okara fall under low values depicted by green color these cities showed results fall on the fitted line. However, by this comparative assessment it was evaluated that mainly major portion of Lahore, Okara and Sheikhupura shows concentrations of PM$_{2.5}$ in the atmosphere are affected by the variance in metrological factors. As the concentrations of PM$_{2.5}$ increased and metrological factors increased so the values in estimate increased, the values of residuals decreased simultaneously. Lahore, Okara, Kasur, and Sheikhupura cities showed results fell between observed and predicted values.

4.7 wind direction and velocity for winter season

Along with the local sources global or transboundary sources are also active for the enrichment of aerosol's concentration. Cross-border pollutants from industrialized countries through natural winds can affect nearby backward countries in terms of additional health care costs and loss of crop productivity because dangerous pollutants in the air can cause dry fog and rain that rains on sulfuric and nitric acid (Okowa, 2000).In the year 1998 winter season the predominant direction is West and Northwest shown in Figure 4.7(a) with maximum velocity of 2.5 ms^{-1} and a minimum velocity of 0.3 ms^{-1}. Medium velocity of wind was observed in Lahore, Kasur, and Okara. While

high wind velocities observed in the Nankana Sahib and Sheikhupura. In the year 2008 winter season the predominant direction is West and Northwest shown in Figure 4.7 (b) with maximum velocity of 2.5 ms^{-1} and minimum velocity of 0.02 ms^{-1}. Medium velocity observed in Lahore, Sheikhupura and some parts of Nankana Sahib while high wind velocity was noted for the Kasur, Okara and most of the Nankana sahib. In the year 2019 winter season the predominant direction is west, and Southwest shown in Figure 4.7 (c) with maximum velocity of 2.2 ms^{-1} and minimum velocity of 0.02 ms^{-1}. In 2019, overall maximum velocity is decreased in Lahore division. Okara shows minimum wind velocity while Lahore, Sheikhupura, Kasur and most of Nankana sahib shows medium to maximum wind velocity. However, wind direction in the study area for all years suggests that the winds are primary carriers of pollutants from Punjab in India Over to the Pakistani side. It was believed by experts that cross-border effects are increasing air pollution over Pakistan (Bashir, 2012). Wind velocity plays a pivotal role in the air degradation of Lahore division as results showed that mainly medium to low wind velocities are observed. Low wind velocity prevents PM$_{2.5}$ and other air pollutants from excluding the atmosphere. Long term PM$_{2.5}$ in the atmosphere mainly serves as precursors for smog formation in Lahore, and other cities are also affected in division.

Table 4.3. Showing correlation between metrological factors and PM$_{2.5}$.

	PM$_{2.5}$	Pressure	Relative Humidity	Surface Downwelling Radiations	Temperature	TOA	Precipitation	Wind speed
PM$_{2.5}$	1	0.268	-0.69*	0.178ns	-0.53*	0.15ns	-0.69*	-0.41*
Pressure	-0.26	1	-0.81	0.83	0.95	0.87	-0.81	0.9
Relative Humidity	0.693	-0.81	1	-0.43	-0.76	-0.42	1	-0.71
Surface Downwelling Radiations	0.178	0.83	0.83	1	0.89	0.99	-0.43	0.87
Temperature	-0.21	0.95	0.76	0.89	1	0.91	-0.76	0.92
TOA	0.15	-0.87	-0.47	0.9	0.91	1	-0.47	0.87
Precipitation	0.69	-0.81	0.1	-0.43	-0.76	-0.47	1	-0.71
Wind speed	-0.21	0.9	-0.71	0.87	0.92	0.87	-0.71	1

Table 4.4. showing coefficients values derived from grass for the year 1998.

	PRESSURE	RELATIVE HUMIDITY	TEMPRATURE	PRECIPITATION	WIND SPEED
b1	0.006799	-1.680110	-9.360398	0.403850	5.97804
Rsq1	0.022236	0.08273	0.182584	0.01713	0.0294
$PM_{2.5}$=-9.36(temperature)1.680(relativehumidity)+0.41(precipitation)+0.0078(pressure)+5.988(wind speed) **n**=15214 **R²**=0.780524 **R²adj**=0.780474					

Table 4.5. showing correlation coefficients for the year 2008.

	PRESSURE	RELATIVE HUMIDITY	TEMPRATURE	PRECIPITATION	WIND SPEED
b1	-0.016123	0.547478	3.136960	0.403850	-16.001735
Rsq1	0.015051	0.019744	0.003550	0.001713	0.035989
$PM_{2.5}$ = 3.13(temperature) +0.54 (relative humidity) +0.44(precipitation)-0.07(pressure)-16.1 (wind speed) n=15294 **R²**=0.80 **R²adj**=0.80					

Table 4.6. showing coefficients values derived from grass for the year 2019.

	PRESSURE	RELATIVE HUMIDITY	TEMPRATURE	PRECIPITATION	WIND SPEED
b1	-0.007212	0.096794	-3.313774	0.403850	-13.693808
Rsq1	0.016795	0.000439	0.014317	0.001713	0.016433
$PM_{2.5}$ = -3.31(temperature) +0.01 (relative humidity) +0.41(precipitation)-0.007 (pressure)-13.7 (wind speed) **n**=15269 **R^2**=0. 81 **R^2adj**=0. 82					

Table 4.7. showing coefficents values derived from the year 1998-2019.

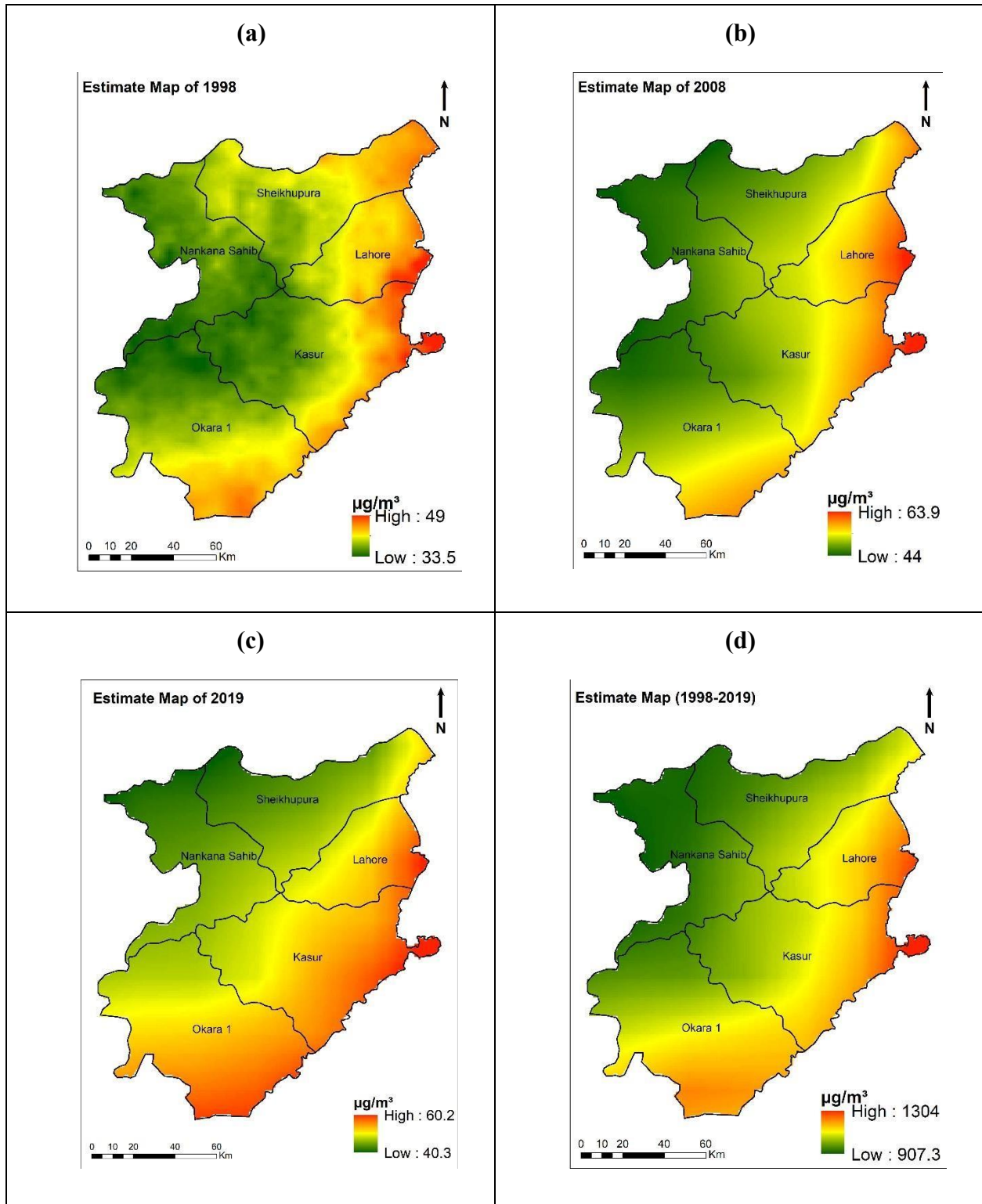|	PRESSURE	RELATIVE HUMIDITY	TEMPRATURE	PRECIPITATION	WIND SPEED
b1	0.001653	0.230509	-1.961992	0.403850	-16.301439
Rsq1	0.000702	0.004405	0.005869	0.001713	0.038856
$PM_{2.5}$ = -1.97 (temperature) +0.23 (relative humidity) +0.41(precipitation)+0.0017 (pressure)-16.3 (wind speed) n=15268 **R^2**=0.85 **R^2adj**=0.85					

Figure 4.5 Displaying estimate map generated from GRASS for the year 1998(a), 2008(b), 2019(c),1998-2109(d).
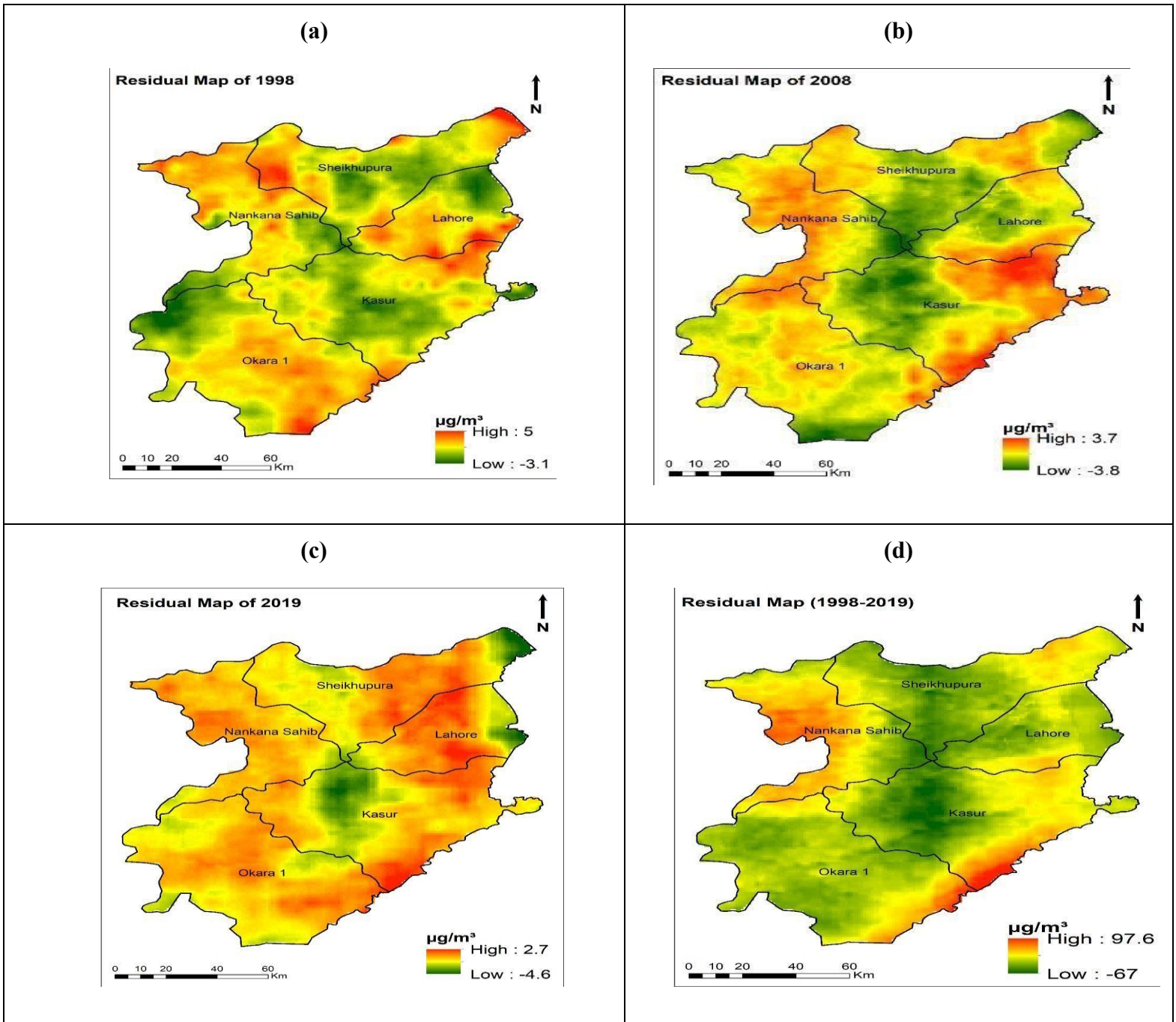
Figure 4.6 Displaying residual map generated from GRASS for the year 1998(a), 2008(b), 2019(c),19982109(d).
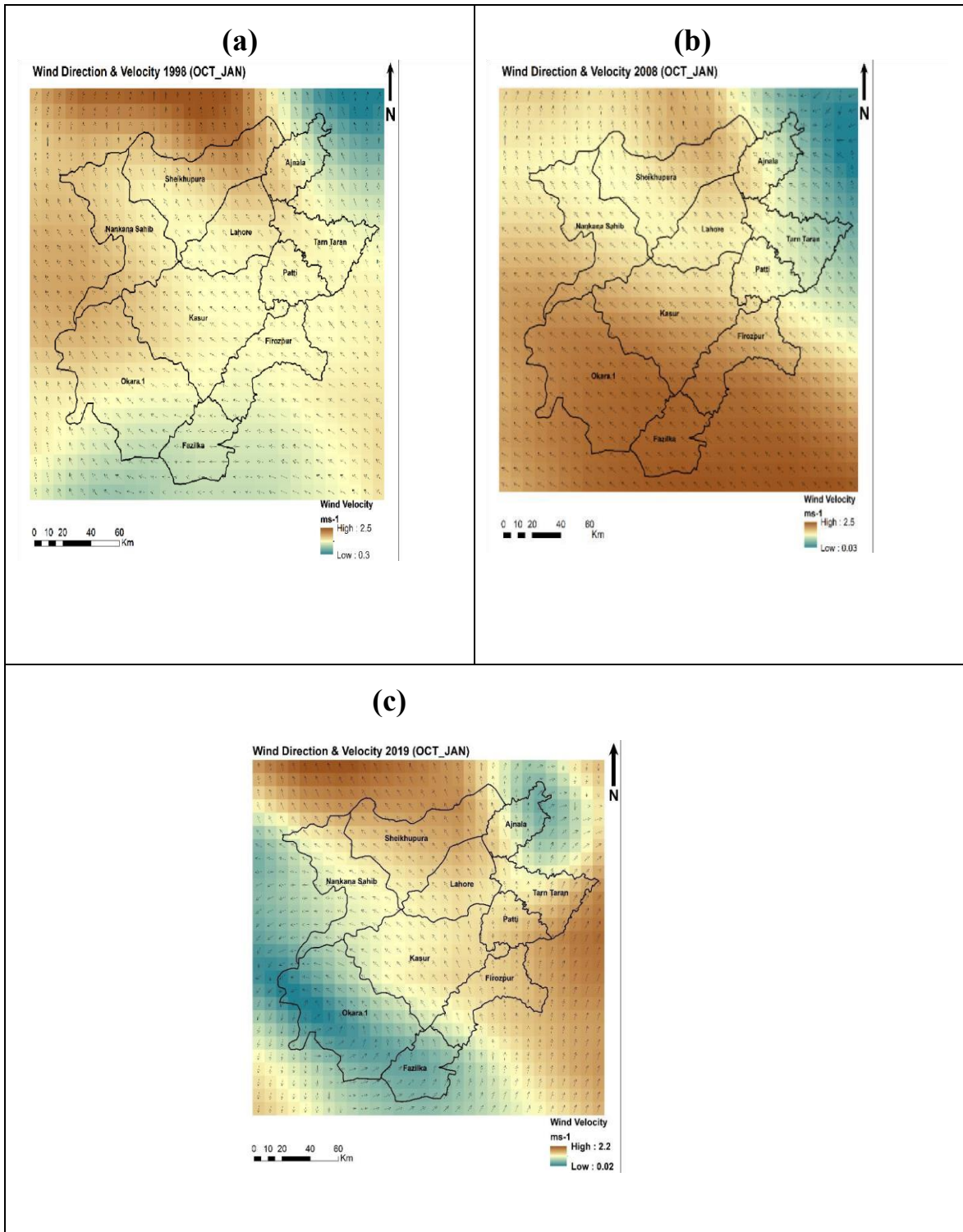
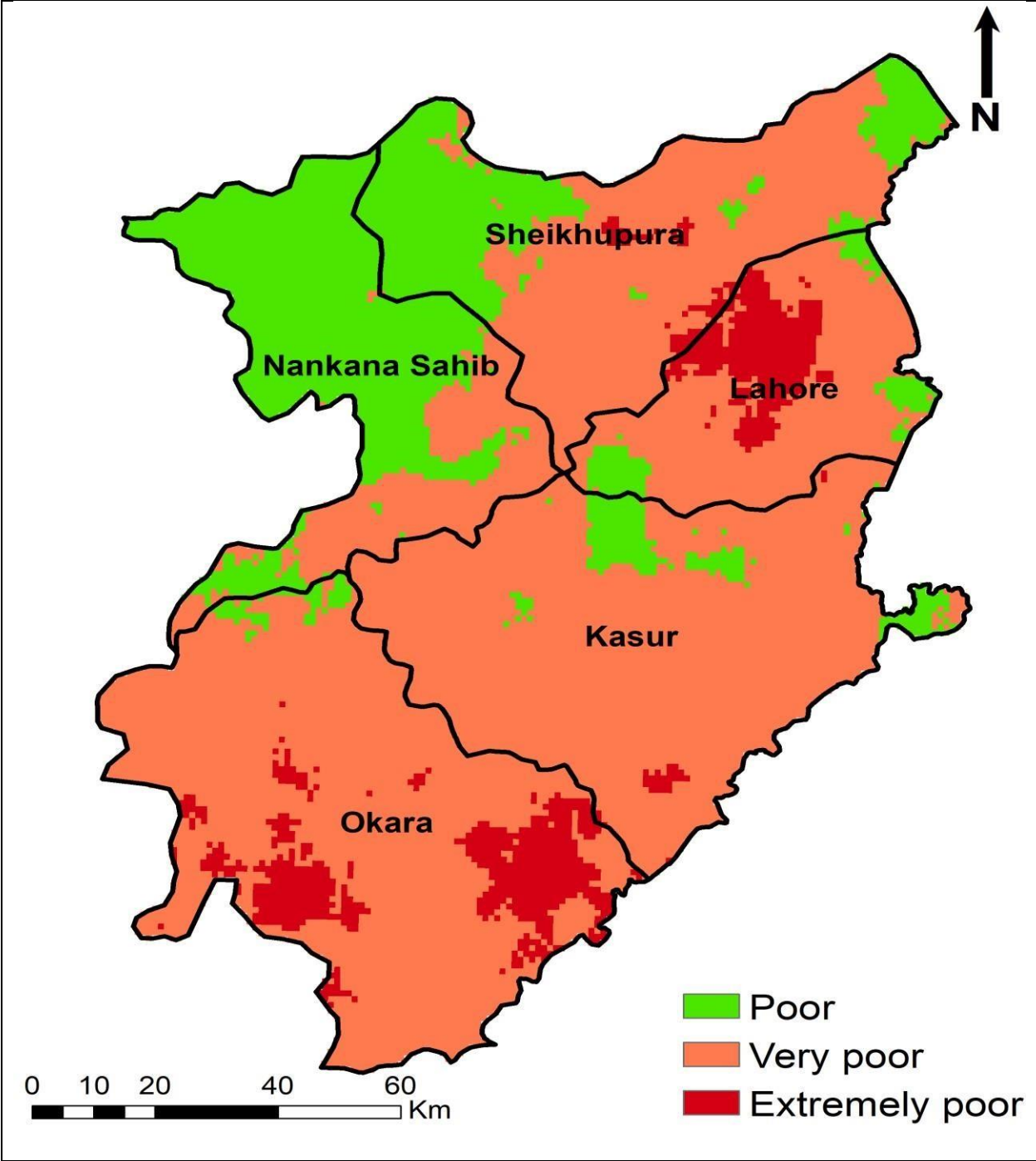Figure 4.7. Presenting prevailing wind direction and magnitude in Lahore division 1998(a),2008(b), 2019(c).

Figure 4.8. Displaying Air Quality in the Lahore division.

Chapter 5

CONCLUSION AND RECOMMENDATIONS

Particulate matter pollution in the Lahore division has drawn much attention in recent years as it has increased significantly over the past few decades resulting in severe impacts on ambient air quality and human health. The study showed that among the Lahore division, the mean annual $PM_{2.5}$ was highest in Lahore during 1998 to 2019. During this period all the cities except Nankana sahib showed an increasing $PM_{2.5}$ trend. Among the Lahore division, air quality was worse in Lahore, Okara, and some parts of Sheikhupura, Kasur ($113ug/m^3$), which was much higher than the WHO ambient air quality standards. It was projected that the population has increased from 1998 to 2019. Therefore, for efficient agricultural production, urbanization and industries are essential to feed and meet the needs of the growing population. $PM_{2.5}$ concentrations are high in Lahore, some parts of Okara, and Sheikhupura because dense urban sprawl and brick kilns, plastic and rubber, rice mill, paper manufacturing, power plants, chemical, wood, leather, steel, metal, textile, and ceramics industries are responsible for particulate matter production. Furthermore, these sources are also present in other cities, but favorable climatic conditions and metrological factors are present in these cities. In addition, wind direction is responsible for accumulating the neighborhood burning residuals in these cities. Wind magnitude is between medium and low, which entrapped $PM_{2.5}$ pollutants in the atmosphere and served as precursors for smog formation in Lahore. Wind magnitude lowers in the winter season, which is why winter is difficult for the people of Lahore, resulting in high mortality rates due to respiratory problems.

Recommendations

Following are the recommendations for this study.

1. More ground stations need to be built in the Lahore division specifically in rural areas and to follow a more even distribution pattern, to increase the accuracy of $PM_{2.5}$ estimation using remote sensing techniques.

2. Pakistan should have cross-border contamination polluter pay laws as have for water contamination.

3. Proper environmental laws and policies should be made and enforced.

4. Industries should use filters in chimneys to combat air pollution.

5. Vehicular emissions could be cut down by using public transport and by promoting afforestation, which helps keep the atmosphere healthy.

References

1. Ahmad, M., Chen, J., Yu, Q., Khan, M. T., Ali, S. W., Nawab, A., . . . Panyametheekul, S. (2023). Characteristics and risk assessment of environmentally persistent free radicals (EPFRs) of PM2.5 in Lahore, Pakistan. *International Journal of Environmental Research and Public Health*, *20*(3), 2384. https://doi.org/10.3390/ijerph20032384

2. Ahmad, M., Cheng, S., Yu, Q., Qin, W., Zhang, Y., & Chen, J. (2020). Chemical and source characterization of PM2.5 in summertime in severely polluted Lahore, Pakistan. *Atmospheric Research*, *234*, 104715. https://doi.org/10.1016/j.atmosres.2019.104715

3. Azimov, U., & Авезова, Н. Р. (2022). Sustainable small-scale hydropower solutions in Central Asian countries for local and cross-border energy/water supply. *Renewable & Sustainable Energy Reviews*, *167*, 112726. https://doi.org/10.1016/j.rser.2022.112726

4. Babu, S. S., Manoj, M. R., Moorthy, K. K., Gogoi, M. M., Nair, V. S., Kompalli, S. K., . . . Singh, D. (2013). Trends in aerosol optical depth over Indian region: Potential causes and impact indicators. *Journal of Geophysical Research: Atmospheres*, *118*(20), 11,794-11,806. https://doi.org/10.1002/2013jd020507

5. Badarinath, K. V. S., Kharol, S. K., Sharma, A. R., & Prasad, V. (2009). Analysis of aerosol and carbon monoxide characteristics over Arabian Sea during crop residue burning period in the Indo-Gangetic Plains using multi-satellite remote sensing datasets. *Journal of Atmospheric and Solar-Terrestrial Physics*, *71*(12), 1267–1276. https://doi.org/10.1016/j.jastp.2009.04.004

6. Badarinath, K. V. S., Sharma, A. R., & Kharol, S. K. (2009). Impact of emissions from anthropogenic sources on satellite-derived reflectance. *Advances in Space Research*,

43(10), 1545–1554. https://doi.org/10.1016/j.asr.2009.01.014

7. Balakrishnan, K., Cohen, A., & Smith, K. R. (2014). Addressing the Burden of Disease

   Attributable to Air Pollution in India: The Need to Integrate across Household and

   Ambient Air Pollution Exposures. *Environmental Health Perspectives*, *122*(1).

   https://doi.org/10.1289/ehp.1307822

8. Bond, T. C., Bhardwaj, E., Dong, R., Jogani, R., Jung, S., Roden, C. A., . . . Trautmann, N.

   M. (2007). Historical emissions of black and organic carbon aerosol from energyrelated

   combustion, 1850–2000. *Global Biogeochemical Cycles*, *21*(2).

   https://doi.org/10.1029/2006gb002840

9. Bräuer, M., Freedman, G., Frostad, J., Van Donkelaar, A., Martin, R. V., Dentener, F., . . .

   Cohen, A. (2015). Ambient Air Pollution Exposure Estimation for the Global Burden of

   Disease 2013. *Environmental Science & Technology*, *50*(1), 79–88.

   https://doi.org/10.1021/acs.est.5b03709

10. Chen, Z., Chen, D., Kwan, M., Chen, B., Gao, B., Zhuang, Y., . . . Xu, B. (2019). The

    control of anthropogenic emissions contributed to 80 % of the decrease in

    PM<sub>2.5</sub> concentrations in Beijing from 2013 to 2017.

    Atmospheric Chemistry and Physics, *19*(21), 13519–13533. https://doi.org/10.5194/acp-

    19-13519-2019

11. Cheng, S., Chen, D., Li, J., Wang, H., & Guo, X. (2007). The assessment of emissionsource

    contributions to air quality by using a coupled MM5-ARPS-CMAQ modeling system: A

    case study in the Beijing metropolitan region, China. *Environmental Modelling and*

    Software, *22*(11), 1601–1616. https://doi.org/10.1016/j.envsoft.2006.11.003

12. Delfino, R. J., Sioutas, C., & Malik, S. (2005). Potential Role of Ultrafine Particles in Associations between Airborne Particle Mass and Cardiovascular Health. *Environmental Health Perspectives*, *113*(8), 934–946. https://doi.org/10.1289/ehp.7938

13. Ding, A., Wang, T., Xue, L., Gao, J., Stohl, A., Lei, H., . . . Zhang, X. (2009). Transport of north China air pollution by midlatitude cyclones: Case study of aircraft measurements in summer 2007. *Journal of Geophysical Research*, *114*(D8). https://doi.org/10.1029/2008jd011023

14. Hartmann, H., & Andresky, L. (2013). Flooding in the Indus River basin — A spatiotemporal analysis of precipitation records. *Global and Planetary Change*, *107*, 25–35. https://doi.org/10.1016/j.gloplacha.2013.04.002

15. He, J., Gong, S., Liu, H., Xu, A., Yu, Y., Zhao, S., . . . Yu, L. (2017). Influences of meteorological conditions on interannual variations of particulate matter pollution during winter in the Beijing–Tianjin–Hebei area. *Journal of Meteorological Research*, *31*(6), 1062–1069. https://doi.org/10.1007/s13351-017-7039-9

16. He, Q., Zhang, M., & Huang, B. (2016). Spatio-temporal variation and impact factors analysis of satellite-based aerosol optical depth over China from 2002 to 2015. *Atmospheric Environment*, *129*, 79–90. https://doi.org/10.1016/j.atmosenv.2016.01.002

17. Hirsch, R. M., Slack, J. R., & Smith, R. A. (1982). Techniques of trend analysis for monthly water quality data. *Water Resources Research*, *18*(1), 107–121. https://doi.org/10.1029/wr018i001p00107

18. Holben, B. N., Eck, T. F., Slutsker, I., Tanré, D., Buis, J., Setzer, A., . . . Смирнов, А. И. (1998). AERONET—A federated instrument network and data archive for aerosol characterization. *Remote Sensing of Environment*, *66*(1), 1–16. https://doi.org/10.1016/s0034-4257(98)00031-5

19. Hu, M., Wang, Y., Wang, S., Jiao, M., Huang, G., & Xia, B. (2021). Spatial-temporal heterogeneity of air pollution and its relationship with meteorological factors in the Pearl River Delta, China. *Atmospheric Environment*, *254*, 118415. https://doi.org/10.1016/j.atmosenv.2021.118415

20. Huang, K., Zhuang, G., Lin, Y., Fu, J. S., Wang, Q., Liu, T., . . . Cao, B. (2012). Typical types and formation mechanisms of haze in an Eastern Asia megacity, Shanghai. *Atmospheric Chemistry and Physics*, *12*(1), 105–124. https://doi.org/10.5194/acp-12-105-2012

21. Jackson, J. M., Hongqing, L., László, I., Kondragunta, S., Remer, L. A., Huang, J., & Huang, H. (2013). Suomi-NPP VIIRS aerosol algorithms and data products. *Journal of Geophysical Research: Atmospheres*, *118*(22). https://doi.org/10.1002/2013jd020449

22. Johnston, F. H., Henderson, S. B., Chen, Y., Randerson, J. T., Marlier, M. E., DeFries, R., . . . Bräuer, M. (2012). Estimated Global Mortality Attributable to Smoke from Landscape Fires. *Environmental Health Perspectives*, *120*(5), 695–701. https://doi.org/10.1289/ehp.1104422

23. Kahn, R. A., Gaitley, B. J., Martonchik, J. V., Diner, D. J., Crean, K. A., & Holben, B. N. (2005). Multiangle Imaging Spectroradiometer (MISR) global aerosol optical depth validation based on 2 years of coincident Aerosol Robotic Network (AERONET)

observations. *Journal* *of* *Geophysical* *Research*, *110*(D10).

https://doi.org/10.1029/2004jd004706

24. Kashif, S., Shah, S. I., & Arooj, F. (2019). Outdoor air quality as influenced by vehicular

exhaust in metropolitan city of Lahore, Pakistan. *Pakistan Journal of Scientific and*

Industrial *Research*, *62*(3), 190–196.

https://doi.org/10.52763/pjsir.phys.sci.62.3.2019.190.196

25. Kaufman, Y. J., Tanré, D., Remer, L. A., Vermote, É., Chu, A., & Holben, B. N. (1997).

Operational remote sensing of tropospheric aerosol over land from EOS moderate

resolution imaging spectroradiometer. *Journal of Geophysical Research*, *102*(D14),

17051–17067. https://doi.org/10.1029/96jd03988

26. Khattak, Babel, & Sharif, M. (2011). Hydro-meteorological trends in the upper Indus

River basin in Pakistan. *Climate* *Research*, *46*(2), 103–119.

https://doi.org/10.3354/cr00957

27. Liang, C. K., West, J. J., Silva, R. A., Bian, H., Chin, M., Davila, Y., . . . Takemura, T.

(2018). HTAP2 multi-model estimates of premature human mortality due to

intercontinental transport of air pollution and emission sectors. *Atmospheric Chemistry and*

Physics, *18*(14), 10497–10520. https://doi.org/10.5194/acp-18-10497-2018

28. Liu, J., Li, J., Zhang, Y., Liu, D., Ding, P., Shen, C., . . . Zhang, G. (2014). Source

Apportionment using radiocarbon and organic tracers for PM2.5 carbonaceous aerosols in

Guangzhou, South China: Contrasting Local- and Regional-Scale Haze events.

Environmental *Science* *&* *Technology*, *48*(20), 12002–12011.

https://doi.org/10.1021/es503102w

29. Lu, K., Fuchs, H., Hofzumahaus, A., Tan, Z., Wang, H., Zhang, L., . . . Zhang, Y. (2019). Fast photochemistry in Wintertime haze: Consequences for pollution mitigation strategies. *Environmental Science & Technology*, *53*(18), 10676–10684. https://doi.org/10.1021/acs.est.9b02422

30. McDuffie, E. E., Smith, S., O'Rourke, P., Tibrewal, K., Venkataraman, C., Marais, E. A., . . . Martin, R. V. (2020). A global anthropogenic emission inventory of atmospheric pollutants from sector- and fuel-specific sources (1970–2017): an application of the Community Emissions Data System (CEDS). *Earth System Science Data*, *12*(4), 3413–3442. https://doi.org/10.5194/essd-12-3413-2020

31. Mishchenko, M. I., & Geogdzhayev, I. V. (2007). Satellite remote sensing reveals regional tropospheric aerosol trends. *Optics Express*, *15*(12), 7423. https://doi.org/10.1364/oe.15.007423

32. Mukhtar, F. (2018). The rising menace of smog: Time to act now. *PubMed*, *30*(1), 1–2. Retrieved from https://pubmed.ncbi.nlm.nih.gov/29504318

33. Na, K., Kumar, K. R., Kang, H., Yu, X., & Yin, Y. (2016a). Long-term (2002–2014) evolution and trend in Collection 5.1 Level-2 aerosol products derived from the MODIS and MISR sensors over the Chinese Yangtze River Delta. *Atmospheric Research*, *181*, 29–43. https://doi.org/10.1016/j.atmosres.2016.06.008

34. Na, K., Kumar, K. R., Kang, H., Yu, X., & Yin, Y. (2016b). Long-term (2002–2014) evolution and trend in Collection 5.1 Level-2 aerosol products derived from the MODIS and MISR sensors over the Chinese Yangtze River Delta. *Atmospheric Research*, *181*, 29–43. https://doi.org/10.1016/j.atmosres.2016.06.008

35. Peng, J., Chen, S., Lu, H., Liu, Y., & Wu, J. (2016). Spatiotemporal patterns of remotely sensed PM 2.5 concentration in China from 1999 to 2011. *Remote Sensing of Environment*, *174*, 109–121. https://doi.org/10.1016/j.rse.2015.12.008

36. Penner, J. E., Dong, X., & Chen, Y. (2004). Observational evidence of a change in radiative forcing due to the indirect aerosol effect. *Nature*, *427*(6971), 231–234. https://doi.org/10.1038/nature02234

37. Raza, W., Saeed, S., Saulat, H., Gul, H., Sarfraz, M., Sonne, C., . . . Kim, K. (2021). A review on the deteriorating situation of smog and its preventive measures in Pakistan. *Journal of Cleaner Production*, *279*, 123676. https://doi.org/10.1016/j.jclepro.2020.123676

38. Reid, J. S., Jonsson, H., Maring, H., Smirnov, A., Savoie, D. L., Cliff, S. S., . . . Tsay, S. (2003). Comparison of size and morphological measurements of coarse mode dust particles from Africa. *Journal of Geophysical Research*, *108*(D19). https://doi.org/10.1029/2002jd002485

39. Remer, L. A., Kaufman, Y. J., Tanré, D., Mattoo, S., Chu, D. A., Martins, J. V., . . . Holben, B. N. (2005). The MODIS Aerosol Algorithm, products, and validation. *Journal of the Atmospheric Sciences*, *62*(4), 947–973. https://doi.org/10.1175/jas3385.1

40. Seinfeld, J. H., Pandis, S. N., & Noone, K. (1998). Atmospheric Chemistry and Physics: From air pollution to climate change. *Physics Today*, *51*(10), 88–90. https://doi.org/10.1063/1.882420

41. Tariq, S., Ul-Haq, Z., & Ali, M. T. (2015). Analysis of optical and physical properties of aerosols during crop residue burning event of October 2010 over Lahore, Pakistan. *Atmospheric Pollution Research*, *6*(6), 969–978. https://doi.org/10.1016/j.apr.2015.05.002

42. Van Donkelaar, A., Martin, R. V., Bräuer, M., Kahn, R. A., Levy, R. C., Verduzco, C., & Villeneuve, P. J. (2010). Global Estimates of Ambient Fine Particulate Matter Concentrations from Satellite-Based Aerosol Optical Depth: Development and Application. *Environmental Health Perspectives*, *118*(6), 847–855. https://doi.org/10.1289/ehp.0901623

43. Wang, Y., Wu, C., Ji, Z., Wang, B., & Liang, Y. (2011). Non-Parametric Change-Point method for differential gene expression detection. *PLOS ONE*, *6*(5), e20060. https://doi.org/10.1371/journal.pone.0020060

44. Yan, D., Ren, X., Kong, Y., Ye, B., & Liao, Z. (2020). The heterogeneous effects of socioeconomic determinants on PM2.5 concentrations using a two-step panel quantile regression. *Applied Energy*, *272*, 115246. https://doi.org/10.1016/j.apenergy.2020.115246

45. Yang, K., Wu, H., Qin, J., Lin, C., Tang, W., & Chen, Y. (2014). Recent climate changes over the Tibetan Plateau and their impacts on energy and water cycle: A review. *Global and Planetary Change*, *112*, 79–91. https://doi.org/10.1016/j.gloplacha.2013.12.001

46. Yokelson, R. J., Crounse, J. D., DeCarlo, P. F., Karl, T., Urbanski, S. P., Atlas, E. L., . . . Shetter, R. E. (2009). Emissions from biomass burning in the Yucatan. *Atmospheric Chemistry and Physics*, *9*(15), 5785–5812. https://doi.org/10.5194/acp-9-5785-2009

47. Yoon, J., Von Hoyningen-Huene, W., Kokhanovsky, A. A., Vountas, M., & Burrows, J. P. (2012). Trend analysis of aerosol optical thickness and Ångström exponent derived from the global AERONET spectral observations. *Atmospheric Measurement Techniques*, *5*(6), 1271–1299. https://doi.org/10.5194/amt-5-1271-2012

48. Zhang, H., Yuan, H., Liu, X., Yu, J., & Jiao, Y. (2018). Impact of synoptic weather patterns on 24 h-average PM2.5 concentrations in the North China Plain during 2013–2017. *Science of the Total Environment*, *627*, 200–210. https://doi.org/10.1016/j.scitotenv.2018.01.248

49. Zhang, J., & Reid, J. S. (2010). A decadal regional and global trend analysis of the aerosol optical depth using a data-assimilation grade over-water MODIS and Level 2 MISR aerosol products. *Atmospheric Chemistry and Physics*, *10*(22), 10949–10963. https://doi.org/10.5194/acp-10-10949-2010

50. Zhang, L., Wilson, J. P., MacDonald, B., Zhang, W., & Yu, T. (2020). The changing PM2.5 dynamics of global megacities based on long-term remotely sensed observations. *Environment International*, *142*, 105862. https://doi.org/10.1016/j.envint.2020.105862

51. Ziomas, I., Melas, D., Zerefos, C. S., Bais, A. F., & Παλιατσός, Α. Γ. (1995). Forecasting peak pollutant levels from meteorological variables. *Atmospheric Environment*, *29*(24), 3703–3711. https://doi.org/10.1016/1352-2310(95)00131-h